NASA

Technical Memorandum 86118

THE Z_3 MODEL OF SATURN'S MAGNETIC FIELD AND THE PIONEER 11 VECTOR HELIUM MAGNETOMETER OBSERVATIONS

J. E. P. Connerney
M. H. Acuna
N. F. Ness

MAY 1984

National Aeronautics and Space Administration

Goddard Space Flight Center
Greenbelt, Maryland 20771

THE Z_3 MODEL OF SATURN'S MAGNETIC FIELD AND THE PIONEER 11 VECTOR HELIUM MAGNETOMETER OBSERVATIONS

J. E. P. Connerney, M. H. Acuña, N. F. Ness,

Laboratory for Extraterrestrial Physics

NASA/Goddard Space Flight Center

Greenbelt, MD 20771

Accepted for Publication by the Journal of

Geophysical Research

May 24, 1984

ABSTRACT

Magnetic field observations obtained by the Pioneer 11 vector helium magnetometer are compared with the Z_3 model magnetic field. These Pioneer 11 observations, obtained at close-in radial distances, constitute an important and independent test of the Z_3 zonal harmonic model, which was derived from Voyager 1 and Voyager 2 fluxgate magnetometer observations. Differences between the Pioneer 11 magnetometer and the Z_3 model field are found to be small ($\sim$ 1%) and quantitatively consistent with the expected instrumental accuracy. A detailed examination of these differences in spacecraft payload coordinates shows that they are uniquely associated with the instrument frame of reference and operation. A much improved fit to the Pioneer 11 observations is obtained by rotation of the instrument coordinate system about the spacecraft spin axis by 1.4°. With this adjustment, possibly associated with an instrumental phase lag or roll attitude error, the Pioneer 11 vector helium magnetometer observations are fully consistent with the Voyager Z_3 model. No evidence is found for any significant departure from axisymmetry of Saturn's internal magnetic field.

INTRODUCTION

In-situ observations of Saturn's magnetic field were obtained by the Pioneer 11 spacecraft in September 1979 and the Voyager 1 and 2 spacecraft in November, 1980 and August, 1981. Pioneer 11, instrumented with a vector helium magnetometer (Smith et al., 1975) and a high-field fluxgate magnetometer (Acuña and Ness, 1975), obtained measurements along a near equatorial trajectory with a closest approach of 1.35 Saturn radii (R_S) . Voyager 1 and 2 hosted identical magnetic field experiments, consisting of dual low-field and high-field fluxgate magnetometer systems (Behannon et al., 1977). Voyager 1 and 2 obtained measurements of Saturn's field at relatively high (north and south) latitudes, approaching to within 3.07 and 2.69 R_S of Saturn, respectively.

Saturn's planetary magnetic field, as measured by Pioneer 11, was found to be well approximated by a dipole of moment 0.2 G-R_S^3. The polarity of Saturn's dipole, like Jupiter's, is opposite to that of the Earth. Most remarkable, however, was the unexpectedly small angular separation ($\lesssim 1°$) of Saturn's magnetic and rotation axes (Smith et al., 1980). In contrast, the Earth and Jupiter have dipole tilts of 11.5° and 9.6°, respectively.

Analyses of the Voyager 1 and 2 magnetometer observations led to an axisymmetric octupole model of Saturn's magnetic field, the Z_3 model (Connerney et al., 1982). This three-parameter model is characterized by the Schmidt-normalized zonal harmonic coefficients g_1^0 = 21535 nT, g_2^0 = 1642 nT and g_3^0 = 2743 nT. The three zonal harmonics proved to be both necessary and sufficient to describe Saturn's planetary magnetic field. No evidence could

be found in the Voyager magnetometer observations of a departure from axisymmetry of the planetary field, at a level of $\sim$ 2 nT ($\sim$ 0.2% of the total field measured at closest approach). The surprising spin symmetry of Saturn's magnetic field was also clearly evidenced in the near-equatorial charged particle observations (Simpson et al., 1980) obtained by Pioneer 11. However, the strong periodic modulation of Saturn kilometric radiation (SKR), upon which the rotation rate of Saturn is based (Desch and Kaiser, 1981), is suggestive of some departure from axisymmetry. This and other reports of periodic phenomena have motivated a continuing evaluation of the Z_3 model and available magnetometer observations.

A number of independent tests of the validity of the Z_3 model have already been conducted. Connerney et al. (1982) fitted zonal harmonic models to the Voyager 1 and 2 data sets, obtaining independent estimates of the g_n^0 coefficients which differed by $\lesssim$ 100 nT. Acuña et al. (1983) demonstrated that the Z_3 model was consistent with each of the charged particle absorption signatures observed in Saturn's magnetosphere, taking into account the small externally-generated field of the ring current (Connerney et al., 1981; Connerney et al., 1983). Connerney et al. (1984), extending the charged particle analyses of Chenette and Davis (1982) to include octupole terms, found the Z_3 model consistent with a zonal harmonic model least-squares fitted to the ensemble of Voyager 2 absorption signatures. In an analysis of charged particle stability in Saturn's ring plane, Northrop and Hill (1983) found that the Z_3 model agreed very accurately with the radial position of the inner edge of the B ring, whereas offset and centered dipole models did not. However, magnetic field models obtained from the Pioneer 11 vector helium magnetometer observations (Smith et al., 1980; Davis and Smith, JPL report, 1983) differed

significantly with the Voyager Z_3 model.

In this note we carefully examine the Pioneer 11 vector helium magnetometer observations as a further evaluation of the Z_3 model and to search for evidence of any departure from axisymmetry of Saturn's magnetic field. Comparison of the Pioneer 11 high field fluxgate observations with either the Z_3 model or the vector helium magnetometer observations is not fruitful because of the relatively large quantization step size of the Pioneer 11 fluxgate magnetometer.

VECTOR HELIUM MAGNETOMETER OBSERVATIONS

The Pioneer 11 vector helium magnetometer observations are most readily displayed in the form of perturbations relative to a model field. These differences, between the Pioneer 11 observations and the field predicted by the Z_3 model, are shown in figure 1 in a spherical coordinate system aligned with Saturn's spin axis for 24 hours of data centered on the time of closest approach. The model perturbation field of Saturn's ring current (Connerney et al., 1983) is indicated by the dashed line; this field of external origin is what we would expect to find in a perturbation plot if we have correctly removed the internal field from 'ideal' observations. Also indicated for each field component are shaded regions representing 1% of the total field magnitude, centered about the model ring current field. The Pioneer 11 vector helium measurements are described as accurate 'at the 1% level' by Smith et al. (1980).

Inspection of figure 1 reveals differences in all three components

between the model field and that observed by the Pioneer 11 vector helium magnetometer. The component discrepancies all increase with increasing field magnitude as Pioneer 11 approached Saturn, generally remaining in magnitude at $\sim$ 1% of the total field. Since the Z_3 model has no ϕ component, the entire ΔB_ϕ plotted is that observed; no model field has been removed. The behavior of the ΔB_ϕ is particularly revealing so we will focus our attention on that component.

Prior to closest approach, from $\sim$ 12 h on day 244 to $\sim$ 16 h, ΔB_ϕ is negative and scales approximately as 1% of the total field magnitude. At $\sim$ 16 h, and prior to closest approach, ΔB_ϕ abruptly reverses sign and approaches again $\sim$ 1% of the field magnitude in the $+\phi$ direction. The ΔB_ϕ component remains at $\sim$ + 1% after Earth occultation (data gap).

Consideration of the spacecraft encounter trajectory illustrated in figure 2 suggests that the behavior of ΔB_ϕ throughout encounter may be a consequence of the Pioneer 11 encounter geometry. In figure 2 we show an equatorial plane projection of the Pioneer 11 encounter from 7 h on day 244 through 2 h on day 245. Pioneer 11 is a spin stabilized spacecraft, rotating about an axis constantly pointed towards Earth as is illustrated in figure 2. Prior to 16 h, day 244, the orientation of the spacecraft spin axis with respect to Saturn is such that it has a component parallel to a radius vector from Saturn. At $\sim$ 16 h, near local dusk, the spacecraft spin axis is perpendicular to the radius vector. Thereafter, through closest approach, Earth occultation, and beyond, the spacecraft spin axis has a component antiparallel to the radius vector. The similarity in the behavior of the ΔB_ϕ and the Saturn-spacecraft geometry suggests that an examination of the

perturbation field in spacecraft coordinates would be instructive.

Spacecraft coordinates are defined in figure 3 as a right-handed Cartesian system oriented with the $\hat{z}$ axis parallel to the spin axis of the spacecraft and directed towards Earth. The spacecraft spin axis must remain within $\sim 1°$ of the spacecraft-Earth vector in order to maintain the Earth within the field of view of the spacecraft antenna (parabolic reflector) for communications purposes. Accurate knowledge of the orientation of the spin axis is obtained by monitoring the amplitude modulation of the strength of the received telemetry signal as the spacecraft spins about its axis. The sense of rotation of the spacecraft is such that the y axis ascends through the ecliptic plane as shown. The x axis completes the right-handed coordinate system.

In figure 4 the perturbation field for 12 h on day 244 through 20 h is replotted in spacecraft coordinates. In this plot, we have removed from the observations the Z_3 model internal field and the small externally- generated field of the ring current that was illustrated in figure 2 with the dashed line. What remains is simply the difference between the vector helium magnetometer observations and the 'expected' model field. The ΔB_Z, along the spacecraft spin axis, is given in an expanded scale for clarity and some information relevant to the detailed operation of the magnetometer (range changing) is included. The scales for ΔB_X and ΔB_Y are identical.

From figure 4 one sees immediately that the difference between the measured and model field is largely confined to the plane perpendicular to the spacecraft spin axis ($\hat{z}$). Even the relatively small difference along the spin

axis, however, is related to the operation of the vector helium magnetometer. The instrument operates in one of eight ranges selected automatically on the basis of the ambient field strength. As the spacecraft approaches Saturn and measures an increasingly larger magnetic field, the instrument steps up into increasingly larger ranges. Marked along the trajectory in the ΔB_Z panel are those instances when the instrument is expected to change ranges on the basis of the field magnitude in the x-y plane. Since Saturn's field was principally southward and largely in the spacecraft spin plane, the instrument range changing was in fact controlled by the spin-plane component. The instrument switches range by changing the amplitude of the sweep field and the feedback current scale factor. Coincident with these range changes, a small step is observed in ΔB_Z, particularly evident as the instrument steps up into the 24,000 nT range as indicated in figure 4. Apparently this range change results in a $\sim$ 16 nT jump in the field measured along the z axis. Note that this is a small fraction of the instrument digitization uncertainty (47 nT) in this range of operation. In-flight calibration is accomplished by application of a stepped field of known magnitude (Smith et al., 1975) so a measurement error along the spacecraft spin axis of less than a quantitzation step cannot be detected in calibration. Clearly, the lack of agreement between the measured and model field along the spacecraft spin axis is consistent with the instrumental uncertainty and not related to the accuracy of the Z_3 model.

The difference between the measured and modeled field in the x-y plane can be largely removed by introducing a small (1.4°) rotation about the spacecraft spin axis. Errors introduced by a small rotation (θ) in the direction of rotation of the spacecraft are given by

$$\Delta B_X = -\sin\theta\ B_Y$$

$$\Delta B_Y = \sin\theta\ B_X$$

where B_Y and B_X are the (measured or modeled) components of the field. The dashed line in figure 4 shows the ΔB_X and ΔB_Y which would result from a -1.4° rotation, that is, a lag of 1.4° about the spin axis. It is extremely unlikely that an error introduced by a lack of knowledge of the internal field would behave as a constant 1.4° phase lag about the spacecraft spin axis (roll attitude error), particularly in view of the changing spacecraft-Saturn geometry throughout encounter. Therefore this difference must be due to a phase error in either the spacecraft coordinate system or in the instrument coordinate system. One possibility concerning the instrument coordinate system is summarized below.

As the spacecraft rotates in a steady magnetic field, the x and y axes of the vector helium magnetometer measure a sinusoid at the spacecraft rotation frequency. The magnetometer output is low-pass filtered prior to sampling and recording. The low-pass filter introduces a phase lag of the output relative to the actual field which is appreciable at the typical spin rate of the Pioneer spacecraft. Neglect of this phase lag in the early analyses of Pioneer 10 Jupiter observations led initially to an error of $\sim$ 3° in the deduced magnetic field orientation, essentially a roll attitude error (Smith et al., 1974), which is precisely the kind of error we seek to explain here. The 3° phase lag introduced by the Pioneer 10 instrument filter resulted from a spacecraft spin period of 12 seconds. Pioneer 11 was spinning appreciably faster at the Saturn encounter, however, with a 7.7 second period. An additional $\sim$ 1.6° phase lag would result since in this frequency range the output response is well approximated by a simple linear phase Butterworth

(Smith et al., 1974). However, this additional 'electronic' phase lag introduced by the increased spacecraft rotation rate has been compensated for in the Pioneer 11 data reduction. Thus the 1.4° phase lag inferred from the comparison of the measured and model field may be due to any (or all) of the following: a small electronic (instrument) phase lag of unknown origin, an uncertainty in the spacecraft roll angle (spin phase), or an uncertainty of the instrument coordinate system referenced to that of the spacecraft.

The attitude of the Pioneer 11 spacecraft is normally obtained from knowledge of the orientation of the spacecraft spin axis and data from a sun sensor. Accurate knowledge of the orientation of the spin axis is obtained by monitoring the amplitude modulation of the strength of the received telemetry signal as the spacecraft spins about its axis. At Saturn encounter, the cone angle of the sun (sun-spacecraft-Earth angle) was very small ($\sim$ 2.5°), resulting in large uncertainties (10-20°) in the spacecraft roll angle determination. These uncertainties were substantially reduced by utilizing data from the Imaging Photopolarimeter (Gehrels et al., 1980) to calibrate the sun sensor. Since no independent determination of the absolute spacecraft roll angle was available, all spin phase measurements are referenced to the Imaging Photopolarimeter coordinate system. Thus an uncertainty of $\sim$ 1.4° in the spacecraft roll angle is not unlikely.

Note that the $\sim$ 460 second oscillations appearing in all three components (see figure 4) are probably beat frequency oscillations, and not physically associated with variations in Saturn's magnetic field. Instead, we suggest that they result from averaging the magnetometer observations over a non-integral number of spacecraft rotations. The averages provided to the

National Space Science Data Center are 60 second averages, which coupled with the 7.7 second spin period, yields an oscillation with a beat period of 7.7 x 60 or ∿ 462 seconds.

CONCLUSIONS

A retrospective analysis of the Pioneer 11 vector helium magnetometer observations has been performed as part of a continuing evaluation of the Z_3 model of Saturn's magnetic field. Small differences between the vector helium magnetometer observations and the Z_3 model field have been identified and attributed to the combined effects of instrument range-changing and a 1.4° roll angle error. Differences between the Z_3 model and models resulting from earlier analyses of the Pionener 11 vector helium magnetometer observations (Smith et al., 1980; Davis and Smith, JPL Report, 1983) are probably largely due to these small measurement errors. When the roll angle error is removed from the observations via a rotation about the spacecraft spin axis, the remaining difference between the observations and the Z_3 model is everywhere less than the discontinuous step error (∿ 0.5%) associated with the instrument autoranging. There remains, therefore, no evidence of any departure from axisymmetry of Saturn's planetary magnetic field nor any evidence of a departure from the Z_3 model.

The accuracy with which the combined Z_3 and ring current model represents the Pioneer 11 vector helium magnetometer observations is remarkable. Independent zonal harmonic models obtained from the Voyager 1 and Voyager 2 data sets (Connerney et al., 1982) differed by < 150 nT in the g_1^0 (21,535 nT)

coefficient and $\lesssim$ 100 nT in the g_2^0 (1,642 nT) and g_3^0 (2743 nT) coefficients. Northrop and Hill's analysis (1983) also suggested that the Z_3 coefficients are accurate to within $\lesssim$ 100 nT. The Pioneer 11 vector helium magnetometer observations, obtained at close-in radial distances (1.35 R_J), also suggest that the field is known and modeled to better than 0.5% at that distance. No departure from axisymmetry is evidenced in any of the in-situ magnetometer data and the enigma of the source of modulation of Saturn's radio emission remains.

ACKNOWLEDGEMENTS

We thank Dr. Ed Smith, Principal Investigator for the Pioneer Vector Helium magnetometer experiment, for helpful discussions and gratefully acknowledge analyses performed by Dr. Ed Smith and his colleagues at the Jet Propulsion Laboratory and Dr. L. Davis, Jr. of the California Institute of Technology.

We thank our Voyager colleagues and our colleagues at the Goddard Space Flight Center for useful discussions, also Frank Ottens, L. White and F. Hunsaker and the data processing and technical support staff at GSFC for their assistance.

FIGURE CAPTIONS

Figure 1: Perturbation magnetic field $\Delta\bar{B}$ observed by Pioneer 11 during Saturn encounter. In this presentation, the Z_3 model internal field has been subtracted from the measurements, in a spherical coordinate system aligned with Saturn's spin axis. The dashed line is the externally generated field of the model ring current. Shaded zone corresponds to 1% of the total field magnitude.

Figure 2: Ring plane projection of the Saturn encounter trajectory. The orientation of the Earthward-pointing spin axis of the Pioneer 11 spacecraft is illustrated near hours 9 and 24, day 244. Hour intervals marked along the trajectory are spacecraft event time, uT.

Figure 3: Pioneer 11 spacecraft coordinate system. The spin axis ($\hat{z}$) is always oriented towards Earth.

Figure 4: Perturbation magnetic field $\Delta\bar{B}$ as in figure 1 but in spacecraft payload coordinates. The Z_3 model internal field and the model ring current field have been subtracted from the measurements.

REFERENCES

Acuña, M. H., and N. F. Ness, The Pioneer 11 High field fluxgate magnetometer, Space Sci. Inst., 1, 177-188, 1975.

Acuña, M. H., J. E. P. Connerney, and N. F. Ness, The Z_3 zonal harmonic model of Saturn's magnetic field: implications and applications, J. Geophys. Res., 88, 8771-8778, 1983.

Behannon, K. W., M. H. Acuña, L. F. Burlaga, R. P. Lepping, N. F. Ness, and F. M. Neubauer, Magnetic field experiment for Voyagers 1 and 2, Space Sci. Rev., 21, 235-257, 1977.

Chenette, D. L., and L. Davis, Jr., An analysis of the structure of Saturn's magnetic field using charged particle absorption signatures, J. Geophys. Res., 87, 5267-5274, 1982.

Connerney, J. E. P., M. H. Acuña, and N. F. Ness, Saturn's ring current and inner magnetosphere, Nature, 292, 724, 1981.

Connerney, J. E. P., N. F. Ness, and M. H. Acuña, Zonal harmonic model of Saturn's magnetic field from Voyager 1 and 2 observations, Nature, 298, 44, 1982.

Connerney, J. E. P., M. H. Acuña, and N. F. Ness, Currents in Saturn's magnetosphere, J. Geophys. Res., 88, 8779-8789, 1983.

Connerney, J. E. P., L. Davis, and D. L. Chenette, Magnetic field models, in Saturn, ed. T. Gehrels, Univ. Arizona Press, in press.

Desch, M. D., and M. L. Kaiser, Voyager measurement of the rotation rate of Saturn's magnetic field, Geophys. Res. Lett., 8, 253-256, 1981.

Gehrels, T., L. R. Baker, E. Beshore, C. Blenman, J. J. Burke, N. D. Castillo, B. DaCosta, J. Degewij, L. R. Doose, J. W. Fountain, J. Gotobed, C. E. KenKnight, R. Kingston, G. McLaughlin, R. McMillan, R. Murphy, P. H. Smith, C. P. Stoll, R. N. Strickland, M. G. Tomasko, M. P. Wijesinghe, D. L. Coffeen, and L. Esposito, Imaging Photopolarimeter on Pioneer Saturn, Science, 207, 434-439, 1980.

Northrop, T. G., and J. R. Hill, The inner edge of Saturn's B ring, J. Geophys. Res., 88, 6102-6108, 1983.

Simpson, J. A., T. S. Bastian, D. L. Chenette, R. B. McKibben, and K. R. Pyle, The trapped radiations of Saturn and their absorption by satellites and rings, J. Geophys. Res., 85, 5731-5762, 1980.

Smith, E. J., L. Davis, Jr., D. E. Jones, P. J. Coleman, Jr., D. S. Colburn, P. Dyal, C. p. Sonett, and A. M. A. Frandsen, The planetary magnetic field and magnetosphere of Jupiter: Pioneer 10, J. Geophys. Res., 79 3501, 1974.

Smith, E. J., B. V. Connor, and G. T. Foster, Jr., Measuring the magnetic fields of Jupiter and the outer solar system, IEEE Trans. Magn., Mag-11, 962, 1975.

Smith, E. J., L. Davis, D. E. Jones, P. J. Coleman, Jr., D. S. Colburn, P. Dyal, and C. P. Sonett, Saturn's magnetosphere and its interaction with the solar wind, J. Geophys. Res., 85, 5655-5674, 1980.

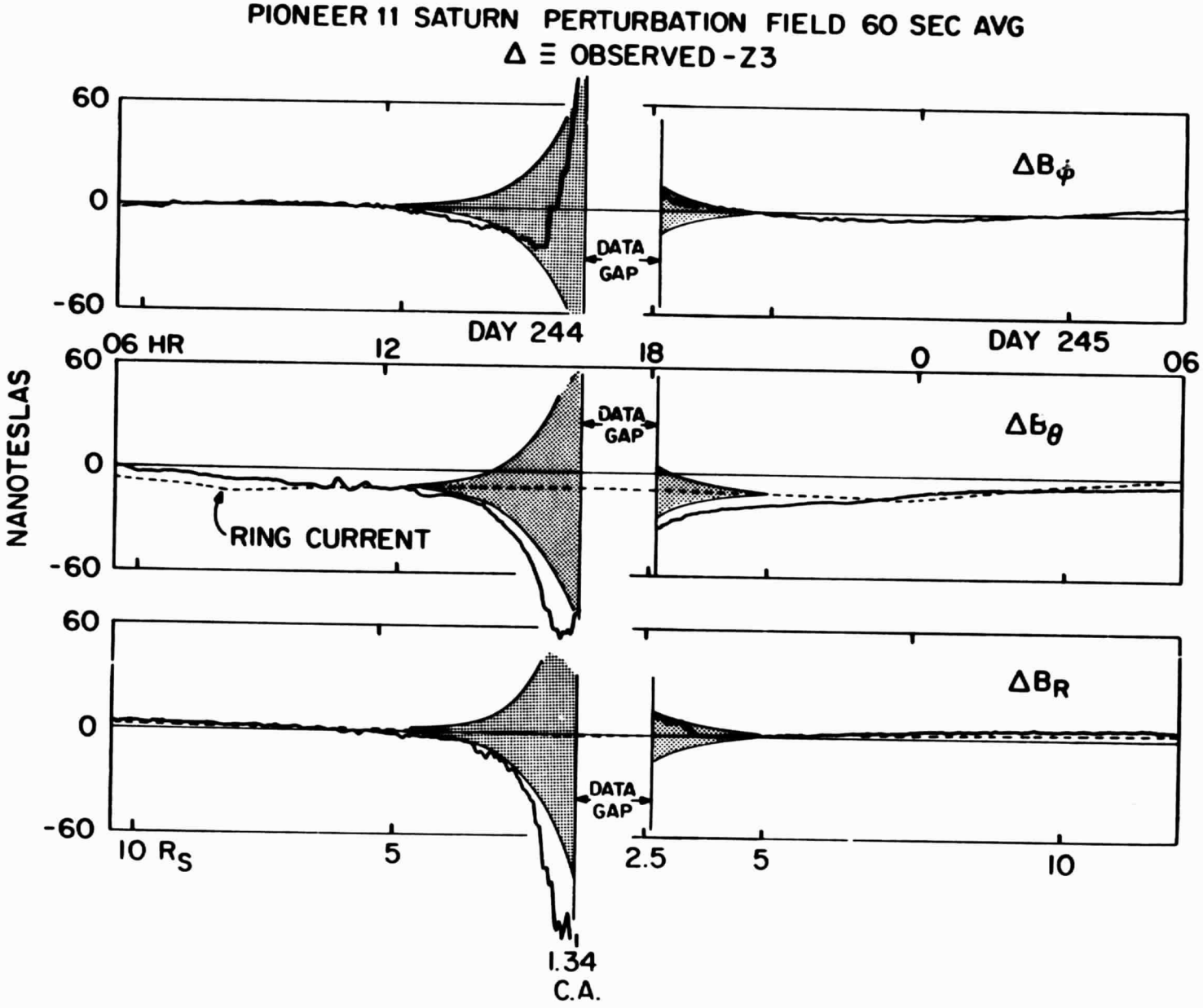

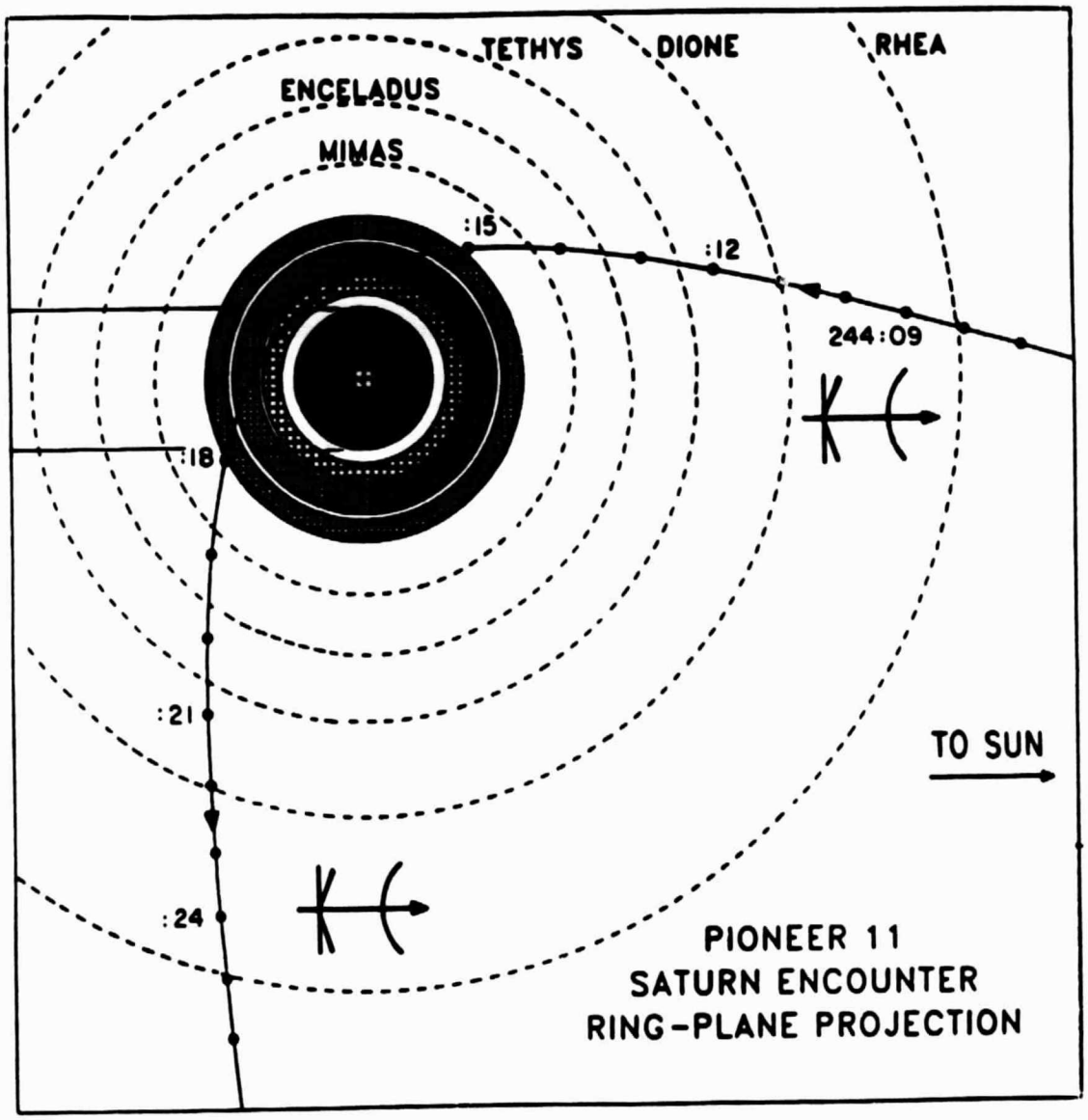

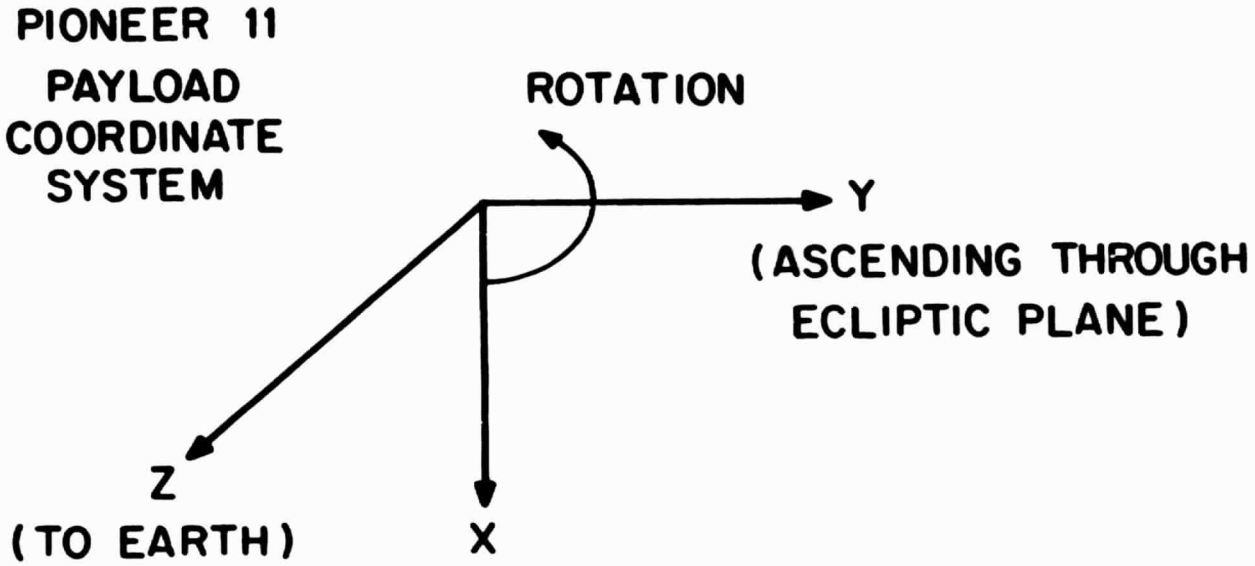
PIONEER 11
PAYLOAD
COORDINATE
SYSTEM
ROTATION
Y
(ASCENDING THROUGH
ECLIPTIC PLANE)
Z
(TO EARTH)
X

PIONEER 11 PERTURBATION FIELD 60 SEC AVG
Δ = OBSERVED - MODEL, PAYLOAD COORDINATES